Wave-induced transport through coastal vegetation

Basic Information

Title:	Wave-induced transport through coastal vegetation
Project Number:	2010LA70B
Start Date:	3/1/2010
End Date:	2/28/2011
Funding Source:	104B
Congressional District:	6th
Research Category:	Climate and Hydrologic Processes
Focus Category:	Sediments, Geomorphological Processes, Wetlands
Descriptors:	None
Principal Investigators:	Heather Smith

Publication

1. Agnimitro Chakrabarti, Heather D. Smith, Dan Cox, Denny A. Albert. Investigation of Turbulent Structures in Emergent Vegetation under Wave Forcing. Presented at Coastal Sediments 2011 in Miami Florida

Problem Description and Research Objectives

The State of Louisiana is facing serious challenges in dealing with coastal erosion and subsidence. The Mississippi River has been hydraulically engineered since the last four decades to suit navigational and economic requirements of the country and this in turn has resulted in massive shortage of sediment supply to Louisiana's wetlands. Further, wave erosion at wetland fringes coupled with a sediment supply rate that is considerably lower than that needed to offset the subsidence along with a massive sea-level rise in the recent years has resulted in the loss of nearly 4900 km^2 of wetlands (Day *et al.,* 2007). Globally, the steady occurrence of natural disasters like the 2004 Indian Ocean Tsunami, Hurricane Katrina, and others have only bolstered the dire need for an ecologically sustainable, cost effective, natural alternative to shoreline protection. Coastal vegetation comes up as an excellent candidate for this purpose (Danielsen *et al.*, 2005, Kathiresan & Rajendran, 2005, Barbier *et al.*, 2008). Vegetation aids in the reduction of energy of incoming waves by turbulent dissipation, commonly called damping. The efficiency of the wave attenuation is significantly more as dissipation occurs not only at the bottom but throughout the entire vegetation height as eddies are generated and shed along the entire stalk. In their field experiment with *Spartina anglica* salt marshes in eastern England, Neumeier and Amos (2006) found that in wave dominated environments, significant attenuation of wave orbital velocity occurring in the denser part of the salt marsh canopy resulting in an effective reduction of 20-35% of the turbulent kinetic energy. The resulting turbulence in the water column is found to control the settling rate of sediments and through a reduction in the bed shear stress limits the bed erosion rate. The vortices generated by the turbulence act as vehicles of exchange for nutrients and manifests biological processes such as dispersion of fish larva. While a considerable number of researchers have worked to quantify the influence of canopy structure in mono-directional current flows in field environments (Leonard and Luther, 1995 and Leonard and Reed, 2002) and in the laboratory with artificial vegetation (Nepf, 1999 and Nepf and Vivioni, 2000), studies in exclusively wave-dominated environments are limited. Koch and Gust (1999) noticed for sea-grass in the field that the vegetation flaps with the wave forcing, producing barriers between the flow and the lower part of the vegetation over part of the wave cycle and an open structure as the wave reverses. This open structure is thought to be an avenue of sediment exchange, but the exact mechanism is unknown. The uncertainty is primarily due to the increased difficulty in getting accurate field measurements of wave forcing within the canopy and also in part due to the difficulty in reproducing a natural canopy in the laboratory flume. Existent work using artificial flexible and rigid vegetation (Augustin *et al.*, 2009) in waves is a first attempt to understand the mechanism. However only a study of a fully natural vegetation canopy can possibly encompass the effects of the structural variety offered by a natural system and can attempt to properly simulate the complex flapping mechanism which plays significant role in turbulent dissipation. The present work is a significant step in this direction as natural vegetation beds of *Schoeneplectus pungens* (bulrush) were used for the present laboratory flume experiments.

The purpose of this project is to quantify the wave-damping capacity of bulrush and to analyze the vertical variation of TKE in order to gain insights into the turbulent structures in play in the water column. In particular the reduction of the observed wave orbital velocities will be studied by comparing with the theoretical LWT values obtained using the wave height data. Energy density spectra for the horizontal and vertical orbital velocities are presented and spectral energies corresponding to the wave component and the turbulent component calculated and their vertical variation within the water column is analyzed.

Objectives

To achieve the project goal, we propose the following specific objectives:

Objective 1: Quantify Wave Damping by Emergent Vegetation

The project will seek to quantify the wave height attenuation over a given distance of vegetation bed. Wave height data collected from wave gauges placed at a given distance apart will be used to calculate the wave height attenuation factor. Both vegetation and vegetation-less channel data will be presented to study the effect of vegetation on the wave field.

Objective 2: Compare Wave orbital velocities in both horizontal and vertical directions at different heights from the bed with the corresponding Linear Wave Theory predicted values obtained from the wave height data

Velocity measurements from Acoustic Doppler Velocity signals at various heights above the bed in the water column will be collected. Linear Wave Theory will be used to calculate the velocities at the same heights from the wave height data collected in Objective 1. A comparison of these values will give an idea of the variation of the orbital velocities due to the effect of the vegetation.

Objective 3: Conduct an analysis of the spectrum of velocity signals to separate the wave component from the turbulent component and calculate the energy corresponding to the wave portion and the turbulent portion

Spectral energy density plots will be obtained from the ADV measurements of velocities at various depths and the dominant frequency corresponding to the wave component will be isolated to separate the turbulence signal. The area under the turbulent energy spectrum will quantify the turbulence intensities at various depths.

Objective 4: Compare Root Mean Square (RMS) velocities of turbulent and wave components of the orbital velocities at various depths and verify the findings of Objective 3

As a final task of the project, a comparison of the root mean square of orbital velocities at various depths will be made in both vegetation and vegetation-less channels to verify the trend in turbulence intensities as observed in Objective 3.

Experimental Description

The species *Schoeneplectus pungens* or bulrush is a fairly common species of wetland vegetation growing throughout the United States. It is a perennial species with the stem having a triangular cross-section for most of the upper part with a circular cross-section at the base. The vegetation used in the experiment were harvested from young natural bulrush beds in the Tillamook Bay of Oregon in the late spring of 2009. The bulrush stems with their root system still intact were cut out in blocks from the inner estuarine regions experiencing low to moderate wave forcing similar to what was simulated in the laboratory. These were then placed in the specially constructed channel boxes and careful preparation was undertaken to sustain their growth throughout the winter of 2009 in the laboratory, under Dr. Albert's supervision and expertise. The purpose of this exercise was to mimic the field conditions in the best possible way.

The wave experiments were performed at the Oregon State University O. H. Hindsdale Wave Research Laboratory in the large-scale wave flume in the summer of 2010. The wave flume is 104 m long, 3.7 m wide and 4.6 m deep. An upgraded programmable hydraulic ram wave-maker capable of generating regular and random waves was used for generating the waves in this experiment.

Wave gauges placed at the wave maker ram location ensured quality control of these offshore parameters throughout the experiment. Four partitioned channels (A, B, C and D in plan view Fig. 1) each measuring 10 m in length and 63.5 cm in width were constructed parallel to each other and extending in the shoreward direction with channel A being the sand channel, channel B and D being vegetation channels with similar vegetation densities (approximately 1200 stems/m^2) and channel C, the restoration channel, having significantly lesser vegetation density. The vegetation heights in channel D ranged mostly between 50-70 cm with approximately 66% of the stems having heights within this height range. The water depth was 40 cm and thus predominantly emergent conditions prevailed. The waves originated at a distance of 57.94 m offshore from the point where the beds started. A series of wave gauges one in each channel were placed at the beginning of each channel (position marked as 0 m in elevation view of Fig. 1). A movable wheel-mounted platform had wave gauges attached to its offshore end and Acoustic Doppler Velocimeters (ADVs, model Nortek) attached to its onshore end (elevation view Fig. 1). Both regular and random waves were considered, with input wave heights (H_s) of 5 cm to 15 cm and wave periods (T_p) of 1.5 to 3 seconds.

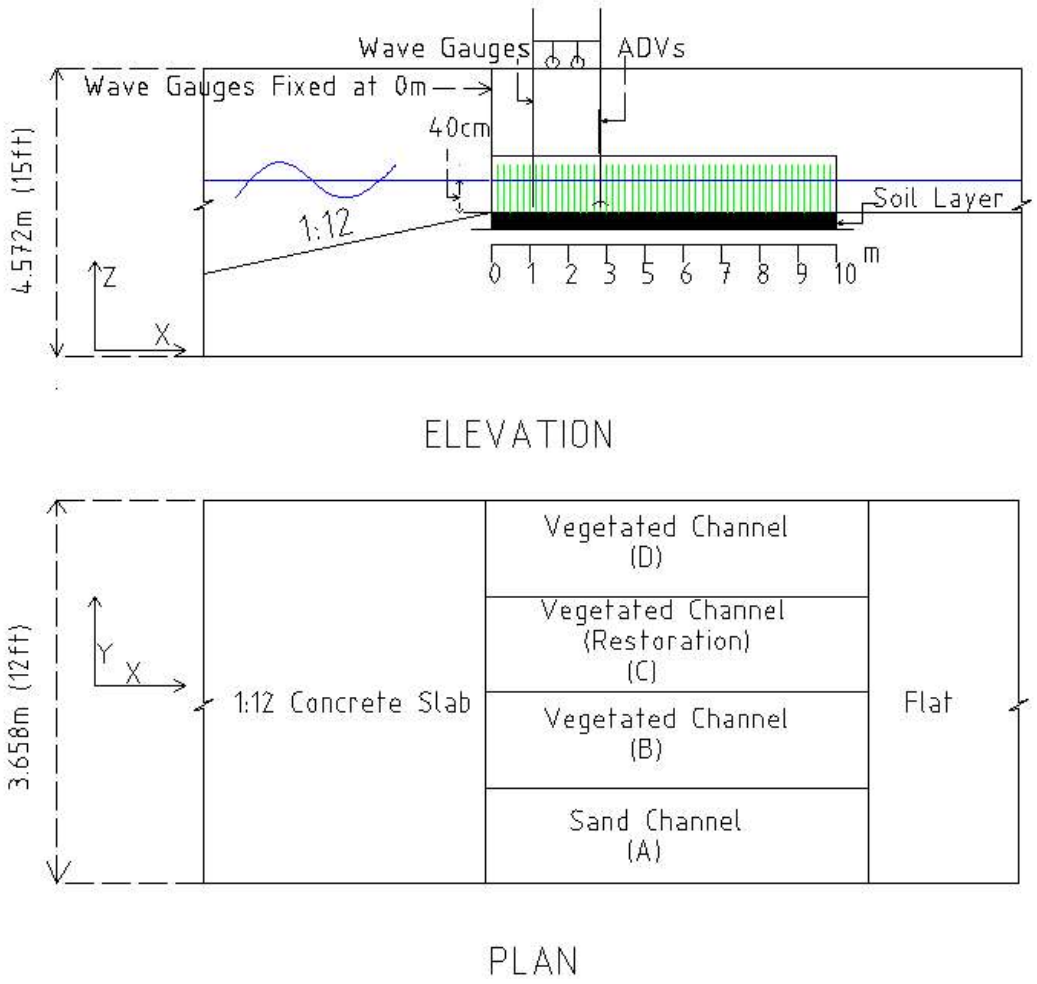

Fig. 1: Experimental setup in the Large Wave Flume. Figure is not to scale.

For the data presented in this report, wave gauges were positioned at x=1.1 m and the ADVs were placed at x=2.9 m in channels A and D (Fig. 2) as these were considered representative for comparing the wave attenuation and resulting turbulence effects in a vegetated channel with a control channel where there is no vegetation. The particular regular wave case presented in this report had H_s = 15 cm and T_p = 1.5 seconds. Wave trains were run in bursts of 120 seconds (2 minutes) and it took on an average 66 seconds for the first wave to reach the 0 m mark while the signal after 105 seconds had effects of the end waves and were often inconsistent. The wave signal between 75 seconds to 102 seconds (18 waves) was found to be completely devoid of any initial and end effects and therefore this

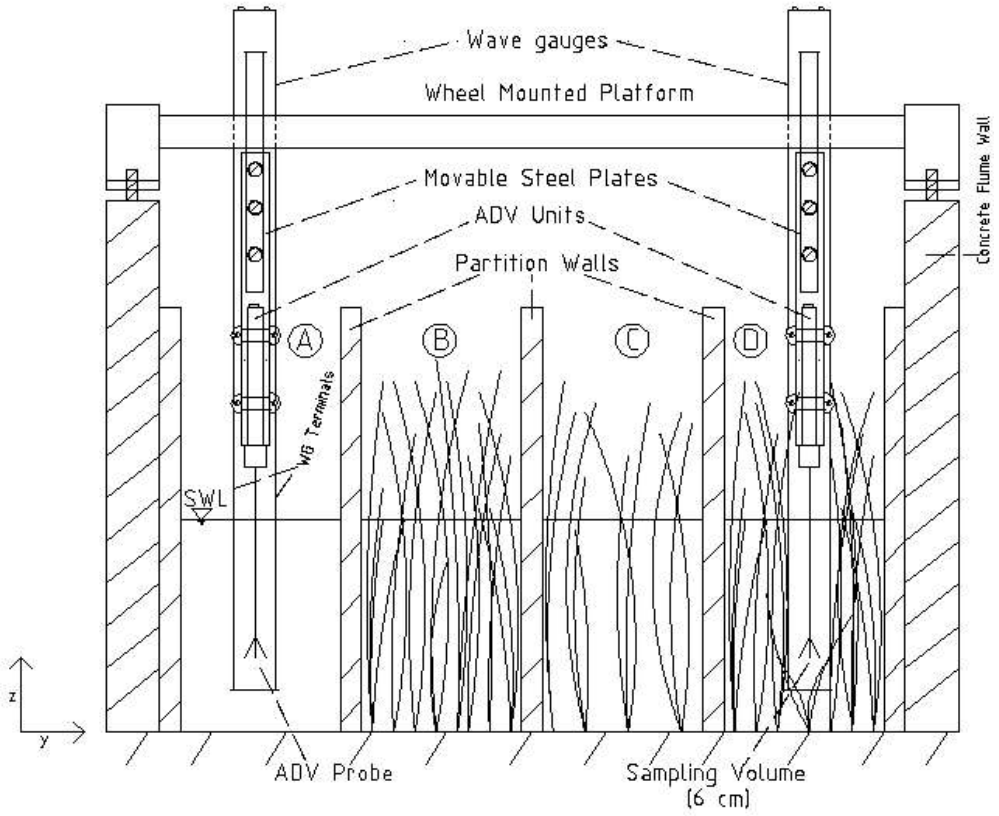

Fig. 2: Cross-sectional view of channels with ADVs and Wave Gauges deployed.

interval has been chosen as the representative interval for all the data presented here. The wave heights, both at 0 m and 1.1 m were computed using a zero crossing method (Tucker and Pitt, 2001) from the wave gauge data. Though precautions were taken to create identical incident wave conditions at the beginning of the channels, post processing of the measured data revealed that the incident wave height at 0 m differed 10-12% from trial to trial for channels A and D and as such it was thought best to acknowledge this experimental variation and present the incident wave height data separately for the two channels. The incident wave heights at 0 m for the two channels were found to be 9.28 cm for the sand channel (A) and 11.41cm for the vegetation channel (D). The wave period was found to remain constant at 1.5 seconds at both x=0 m and x=1.1 m locations implying no significant frequency shift in the waves. The depths of the channels were noted as 42.5 cm for the sand channel and 36.3 cm for the vegetation channel at the ADV location of x=2.9 m. Based on these estimates the incident waves can be considered to be weakly non-linear and use of linear wave theory in estimating the orbital velocities at the study point is not expected to introduce significant errors. A study of the wave transmission coefficients at different points in the vegetated channel from a previous experiment revealed that the variation of wave heights between 1.1 m and 2.9 m was less than 15%. Therefore the use of x=1.1 m wave gauge data to calculate wave orbital velocity values using linear wave theory at x=2.9 m is considered acceptable as a first attempt. The vertical locations of the ADV were

varied from -12.4 cm to -40.4 cm for the sand channel and -12.4 cm to -34.4 cm for the vegetation channel, with the vertical heights being measured from the still water surface at 2 cm increments.

Methodology

Free surface water level elevations were calculated using wave gauges placed in the vegetated and sand channel. The wave heights are computed using the zero crossing method (Tucker and Pitt, 2001) from the elevations data for both the locations in the two channels. Wave height decay is quantified using the wave transmission coefficient $K(x)$ which is defined as a function of wave height $H(x)$ (Dalrymple *et al.*, 1984) as

$$K(x) = \frac{H(x)}{H_0} \quad \text{(1)}$$

where H_0 is the incident wave height and x is the shoreward distance from the incident wave height location.

In order to compare the measured wave orbital velocity data with that predicted by linear wave theory, the theoretical horizontal (u) and vertical (w) velocities were computed using the observed free surface elevation from the wave gauges at as follows,

$$u(t) = \eta(t)\frac{\cosh k(z+d)}{\sinh(kd)} \quad \text{(2)}$$

$$w(t) = \eta(t)\frac{\sinh k(z+d)}{\sinh(kd)} \quad \text{(3)}$$

where $\eta(t)$ is the water surface elevation time series obtained from the wave gauge readings at x=1.1 m; d=the water depth; k=2π/L=wave number where L=wavelength calculated iteratively using the dispersion relationship $L=L_0 tanh(kd)$ where $L_0=gT^2/2\pi$=deepwater wavelength, T being the wave period.

The observed velocities were obtained by de-spiking the ADV data using the method of Mori *et.* al (2007). The missing data points in the de-spiked data set were then obtained using linear interpolation from the nearest neighbor data points. The velocity time series was time synchronized for all the trials using a cross-correlation technique so as to represent the same time window for every trial.

The spectral density (S) was computed with a Fast Fourier Transform algorithm using two ensemble averages and one band average with four degrees of freedom. The spectral energies corresponding to the wave component (Eu or Ew) and the

turbulent component (Eu_t or Ew_t) were separated using these cutoff frequencies, and the spectral energies are defined as,

$$Eu = \tfrac{1}{2}\rho\int_{f_1}^{f_2} S_u(f)df \quad \text{..... (4)}$$

$$Eu_t = \tfrac{1}{2}\rho\int_{f_2}^{f_n} S_{ut}(f)df \quad \text{..... (5)}$$

where, ρ = density of water (10^3 Kg/cu.m), f_n = Nyquist frequency, with Su and Su_t being the spectral densities for the wave component and the turbulent component respectively.

Results and Discussions

The variation of the free surface elevation with time at the initial position (x=0 m) and at the x=1.1 m wave gauge location for both the sand (channel A, top panel) and vegetation (channel D, bottom panel) channels are shown in Fig. 3. Both the sand and the vegetated channels show attenuation of the incoming wave height with the attenuation in the vegetation channel being significantly higher.

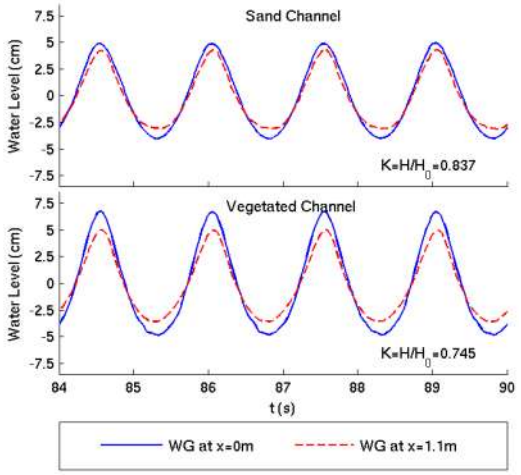

Fig. 3: Wave attenuation by vegetation. The sand channel (channel A) is shown in the top panel, and the vegetated channel (channel D) is shown in the bottom panel. The solid blue line is the incoming wave and the dashed red line is the wave observed 1.1 m into the channel. The wave transmission coefficient is shown for each case.

Using Eqn. (1) the wave transmission coefficients are calculated for each channel, with a wave transmission coefficient of 0.837 for the sand channel and 0.745 for the vegetated channel. The lower value of K(x) in the vegetated channel shows a greater attenuation of the incident waves by the vegetation and yields an increase of 11% in the reduction of the incoming wave over just 1 m of vegetation.

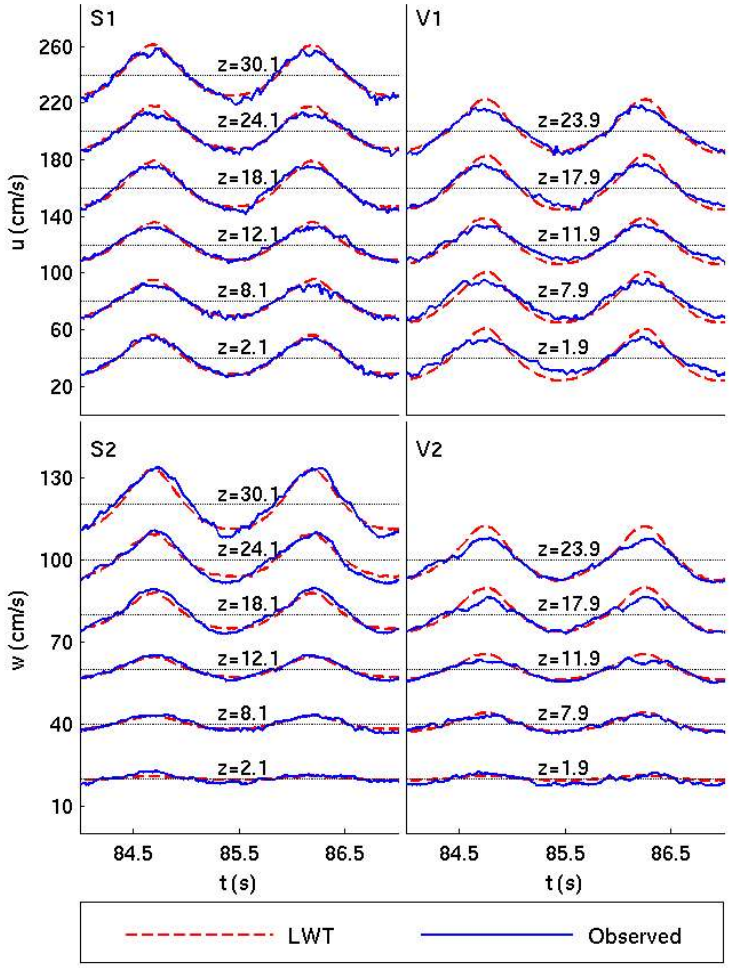

Fig. 4: Comparison of horizontal (u) and vertical (w) components of the wave orbital velocities (solid blue line) in the sand channel (panels S1 and S2) and the vegetation channel (panels V1 and V2) with those predicted by Linear Wave Theory (LWT, dashed red line) calculated from the wave gauge data. Here z represents height in cm from the bed and each elevation is offset by 40 cm/s for panels S1 and V1 and 20 cm/s for panels S2 and V2.

Fig. 4 presents the comparison of the orbital velocity components in both channels with those predicted by LWT at different heights from the bed. It is seen that the observed orbital velocity signatures follow more or less the LWT profiles for the sand channel, while those in the vegetation channel show pronounced variation from the LWT profiles. The deviation is particularly prominent at lower depths for the horizontal component with the linear wave theory predicting higher values. For the vertical component however the variation is more discernible in the upper part of the water column, where the vertical velocities are larger.

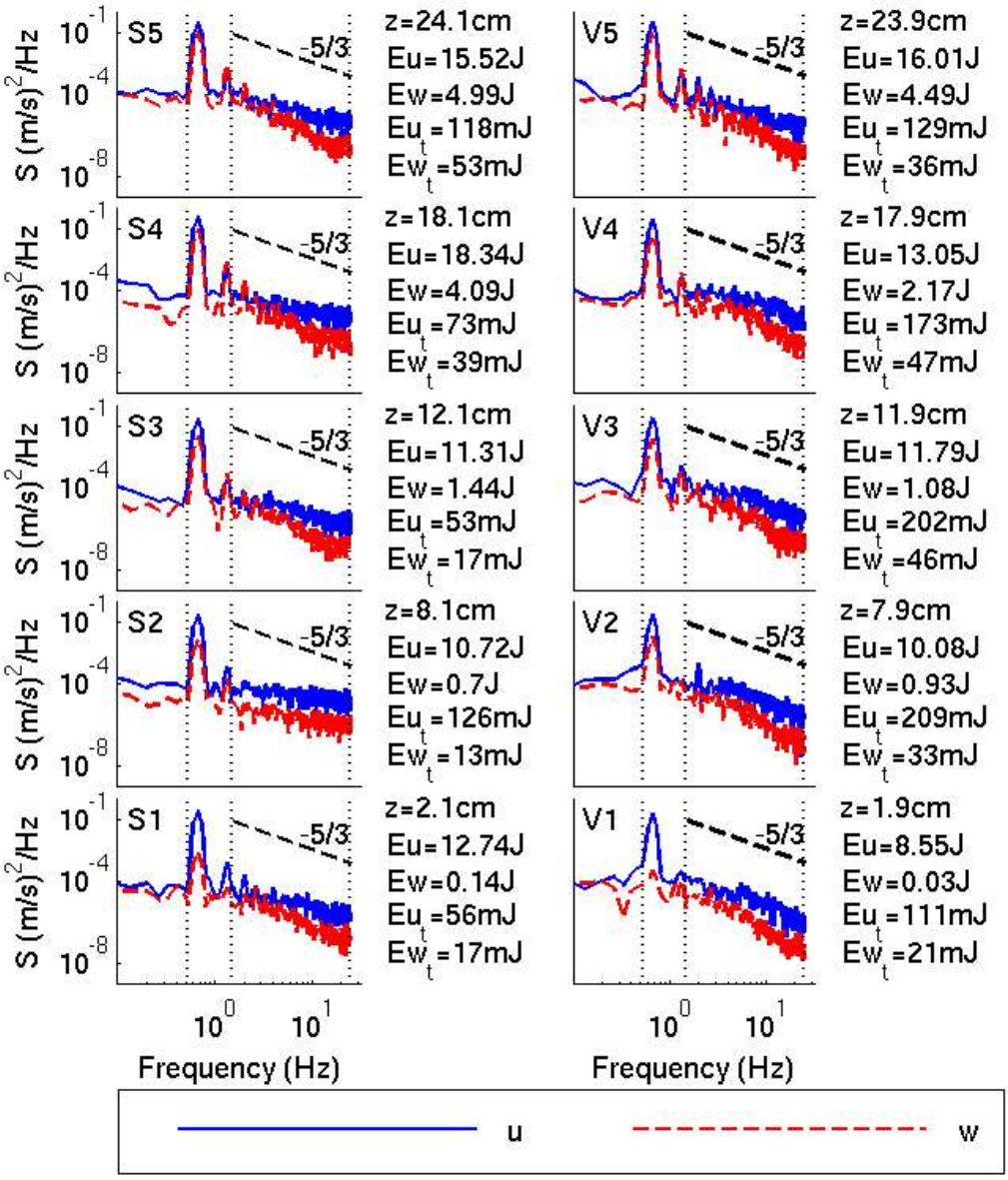

Fig. 5: Power spectra of the horizontal (u, blue solid line) and vertical (w, red dashed line) orbital velocity obtained from the ADV data at different heights (z) above the bed. Eu and Ew are the spectral energies for the wave component while Eu_t and Ew_t are the spectral energies for the turbulent component. S is the spectral density. The vertical dotted lines correspond to the lower and higher cutoff frequencies for the wave component and the Nyquist frequency.

Fig. 5 shows the distribution of the spectral density for the horizontal and vertical velocity components of the observed wave orbital velocity at different elevations above the bed for both sand and vegetated channels. Power spectra plots for all the vertical positions were investigated and the average lower (f_1) and higher (f_2) cutoff frequencies for the wave component of the velocity were found to be 0.531 Hz and 1.492 Hz, respectively as shown with the dotted lines on Fig. 5. Small variations of these frequencies were not found to have any significant effect on the

results. The inertial sub range denoted by the dashed line approximates the slope of the -5/3 line in the log-log scale (Soulsby, 1983) for the vegetation channel. The spectral energies for the wave component (Eu and Ew) decrease with depth for the vegetation channel with the vertical component almost vanishing near the bed, while for the sand channel the Eu value remains fairly invariant while the Ew value decreases with depth indicating the characteristic reduction of the vertical component of the orbital velocity. The turbulent spectral energies are significantly higher for both the velocity components in the vegetation channel than those in the sand channel. Vertical variations reveal that Eu_t and Ew_t show a steady decline with depth from the free surface for the sand channel except for an outlier value of Eu_t (possibly due to imperfections in the ADV measurement) at the z=8.1 cm location from bed. On the other hand, for the vegetation channel, Eu_t increases with depth from the free surface up to about the z=6 cm location from the bed. Ew_t also shows a somewhat similar trend except the decrease appears at a shallower depth of about z=8 cm from the bed. From these spectral energy plots we may say that the maximum reduction of the orbital velocity occurs between 8 to 24 cm that is approximately between the one-fourth to two-third part of the depth, possibly due to increased above ground biomass content within this region.

The vertical distribution of the root-mean-squared (RMS) velocities for the total, wave, and turbulent components are presented in Fig. 6. Panels S1 and V1 show the RMS velocities for the total velocity (u_{rms} and w_{rms}) for the sand and vegetated channels, respectively. The total wave orbital velocity component is defined as $u=u_w+u_t$, where u_w=frequency filtered component containing the effect of the mean wave action only and u_t=turbulent component corresponding to the inertial sub-range of the frequency spectrum. For the sand channel, it is seen that the horizontal component almost matches the linear wave theory value consistent with the velocities shown in Fig. 4. However, the vertical component is higher throughout the depth, and may be attributed to the sensitivity of the vertical velocity to the differences in the actual wave height occurring at the x=2.9 m position with the measured values at x=1.1 m from which the LWT velocities are calculated. For the vegetated channel, it is observed that the vertical velocity component remains generally lower than the LWT estimate in the upper two-third portion of the water column implying greater turbulence reduction. No such consistent profile is however observed for the horizontal component.

Panels S2 and V2 in Fig. 6 present the RMS velocities of wave component ($u_{w,rms}$, $w_{w,rms}$). While the general trends of the vertical profile follow a similar nature for both sand and vegetated beds, the vegetated channel velocities shows an appreciable decrease in the vertical orbital velocity due to dissipation. Consistent with the spectral energies calculated in Fig. 5, most of the total energy is contained in the mean wave energy. The vertical distribution of the RMS of the turbulent component of the orbital velocities ($u_{t,rms}$ and $w_{t,,rns}$) are shown in panels S3 and V3. Both the horizontal and vertical components of the RMS values of the turbulent components in the vegetated channel exhibit a decrease with height from the bed, while the observations in the sand channel do not. At lower elevations, the

turbulent components of the horizontal velocities are much higher than those observed in the sand channel, indicating increased turbulence generation at higher vegetation density (increased vertical biomass). This is consistent with the previous observations from the spectral energy values in Fig. 5. The spike in turbulence at approximately z=15 to 20 cm is likely due to a local change in the vertical distribution of the biomass and needs to be further looked into in correlation with vertical biomass distributions in future publications. This is

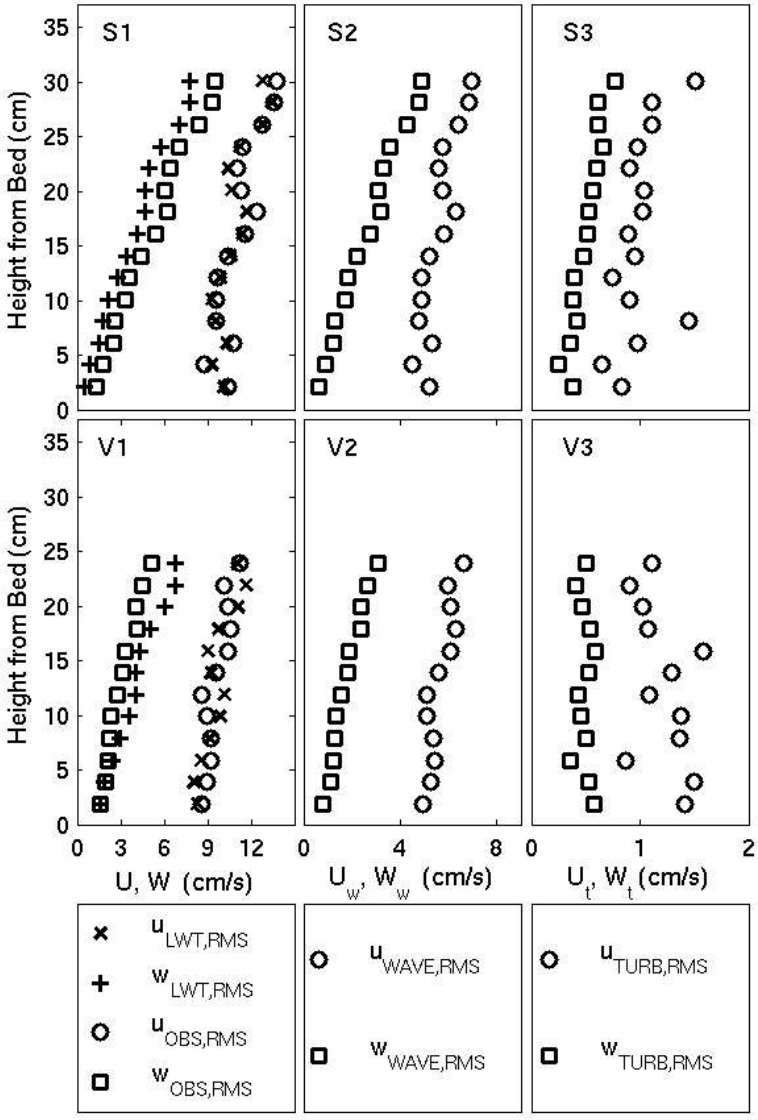

Fig. 6: Comparison of root-mean-squared (RMS) velocities with depth. Panels S1 and V1 present the RMS of the total velocity, panels S2 and V2 present the RMS of the wave velocitiy and panels S3 and V3 present the RMS of the turbulent velocities. Top panels (S1, S2, S3) are distributions for the sand channel and bottom panels (V1, V2, V3) for the vegetated channel. Please note the velocity scale difference in these panels.

consistent with the observations of Neumeier and Amos (2006) who found a spike in observed three-dimensional Reynold's stresses between this range for fully submerged Spartina canopies. The turbulent vertical velocity magnitudes are similar between the vegetated and sand channels. Though the relative scatter in these figures are higher than the previous ones, still it gives an understanding into the dynamics of turbulence distribution within the canopy.

Conclusions

Regular wave cases with significant wave heights and wave periods typical of estuarine conditions were run over two parallel beds, one containing only sand and the other a particular species of bulrush under emergent conditions in the Large Wave Flume at Oregon State University. Wave attenuation effects of the vegetation channel was found to be superior, the wave transmission coefficient for the vegetated channel being 11% lower than that of the sand channel over just the first 1 m of vegetation alone. ADV measurements were obtained and the de-spiked wave orbital velocities after proper time synchronization between the trials were compared to the linear wave theory predicted values, obtained from water surface elevation data from wave gauges at a nearby point. The vertical component of the velocity in the vegetation channel showed greater agreement at the lower water depths with those predicted by LWT, while the horizontal profiles matched the LWT trends in the upper part of the water column. The observed velocity profiles showed close agreement with the LWT profiles for the sand channel.

The power spectra for the orbital velocity components suggests the horizontal and vertical turbulent spectral energies in the vegetation canopy are higher between 10 to 24 cm from the bed with the values decreasing with height from the bed. However no such general trend is observed in the sand channel indicating this is a property of the above ground biomass distribution. As a future scope for work, the correlation of this distribution of the turbulent kinetic energy with the above ground biomass distribution will be studied. The vertical variation of root-mean-squared (RMS) velocities show that for the vegetated channel, the upper half of the water depth exhibits marked reduction in turbulence thereby confirming the earlier finding from the spectral energy values. The turbulence signal for the horizontal velocity component in the vegetated channel is higher than that for the sand channel, yielding increased wave dissipation, but also may affect the dynamics of suspended sediment in the layer. It is worthwhile to point out that during the course of these experiments no discernible sediment movement was observed on the bed, except the formation of minor dunes and troughs.

This work was presented at the 2011 Coastal Sediments Conference in Miami, Florida in May of 2011. One graduate student, Agnimitro Chakrabarti, was supported under this work.

References

Augustin, L.N., Irish, J.L., and Lynnet, P. (2009). "Laboratory and numerical studies of wave damping by emergent and near-emergent wetland vegetation," *Coast. Eng.,* 56(3):332-340.

Barbier, E., Koch, E., Silliman, B., Hacker, S., Wolanski, E., Primavera, J., Granek, E., Polasky, S., Aswani, S., Cramer, L., Storms, D., Kennedy, C., Bael, D., Kappel, C., Perillo, G., and Reed, D. (2008.) "Coastal ecosystem-based management with nonlinear ecological functions and values," *Science 319:5861.*

Dalrymple, R.A., Kirby, J.T., Hwang, P.A. (1984). "Wave refraction due to areas of energy dissipation," *J. Waterw., Port Coast. Ocean Eng*. 110(1):67-69.

Danielsen F., Sorensesn, M.K., Olwig, M.F., Selvam, V., Parish, F., Burgess, N.D., Hiraishi, T., Karunagaran, V.M., Rasmussen, M.S., Hansen, L.B., and Suryadiputra, N. (2005). "The Asian Tsunami: A protective role for coastal vegetation," *Science* 310:643.

Day, J.W., Boesch, D.F., Clairain, E.J., Kemp, P., Laska, S.B., Mitsch, W.J., Orth, K., Mashriqui, H., Reed, D. J., Shabman, L., Simenstad, C.A., Streever, B.J., Twilley, R.R., Watson, C.C., Wells, J.T., and Whigham, D.F. (2007). "Restoration of the Mississippi delta: Lessons from Hurricanes Katrina and Rita," *Science*, 315:1,679-1,684.

Kathiresan, K., and Rajendran, N. (2005). "Coastal mangrove forests mitigated tsunami," *Estuar Coast Shelf Sci* 65:601-606.

Koch, E. and Gust, G. (1999). "Water flow in tide- and wave-dominated beds of seagrass thallasia testudinum," *Mar. Ecol.*, 184:63-72.

Leonard, L.A. and Luther, M.E. (1995). "Flow hydrodynamics in tidal marsh canopies," *Lim. Ocean., 40:1474-1484.*

Leonard, L.A. and Reed, D.J. (2002). "Hydrodynamics and sediment transport through tidal marsh canopies," *J.Coast. Res., SI 36:459-469.*

Mori, N., Suzuki, T., Kakuno, S. (2007). "Noise of acoustic doppler velocimeter data in bubbly flows," J. *Eng. Mech., 133(1):122-125.*

Nepf, H.M. (1999). "Drag, turbulence, and diffusion in flow through emergent vegetation," *Water Res. Res., 35(2):479-489.*

Nepf, H.M. and Vivoni, E.R. (2000). "Flow structure in depth limited, vegetated flow," *J. Geophys. Res., 105(C12): 28547-28557.*

Neumeier, U. and Amos, C.L. (2006). "Turbulence reduction by the canopy of coastal spartina salt marshes," *J. Coast. Res., SI 39:433-439.*

Soulsby, R.L. (1983). “The bottom boundary layer of shelf seas,” John, B. (ed), *Physical oceanography of coastal and shelf seas, Elsevier Ocean. Series*: 189-266.

Tucker, M.J. and Pitt, E.G. (2001). “Waves in ocean engineering,” Amsterdam, Elsevier, 521 p.